Effect of Ferrochrome Addition on Wear and Hardness Properties of Grey Cast Iron

Yusuf O. Busari[1*], Jeleel A. Adebisi[1], Yusuf L. Shuaib-Babata[1], Lukman O. Amuzat[1] and Halimah F. Babamale[2]
[1]Materials and Metallurgical Engineering Department
[2]Industrial Chemistry Department
University of Ilorin
Ilorin, Nigeria
[*]*busari.oy@unilorin.edu.ng*

Date received: July 23, 2020
Revision accepted: November 18, 2021

Abstract

The use of a pair of grinding discs in a domestic milling machine for food processing is commonly practiced in sub-Saharan Africa. During the milling machine operation, the pair of grinding discs wears off gradually by shear and produces metallic particles that contaminate the processed food. This study aimed to reduce these metallic impurities by adding chromium (Cr) to the melt in producing discs to increase the discs' toughness and wear resistance. Cr in the form of ferrochrome (FeCr) was added in weight percentage of grey cast iron to produce alloyed specimens. The control specimen was produced from 40% grinding disc and 60% engine block scraps. Four other experimental specimens were added with FeCr to increase the amount of Cr in subsequent castings. The specimens were prepared and subjected to compositional, phase and microstructural analyses, and hardness and wear resistance tests. The results showed that percentage variations of FeCr in the casts had significant effects on the properties investigated. The addition of FeCr to the melt increased the wt.% amount of Cr and intensity of the phases in X-ray diffractometer patterns for the alloyed cast irons. An increase in the amount of Cr led to an increase in hardness and a reduction in wear rate. Consequently, about 67% reduction wear rate index with moderate hardness was observed in the alloyed casts than the control sample. Thus, the addition of FeCr produced alloyed specimens that would lessen the number of metallic contaminants and frequency of regrooving the grinding discs.

Keywords*:* ferrochrome, grey cast iron, grinding disc, hemochromatosis, wear resistance

1. Introduction

In sub-Sahara Africa, food processing operations include harvesting, cleaning of food materials, sorting, grading, screening, size reduction and preservation.

Traditional methods for grinding consist of using stones and bricks or pestle and mortar. These methods are effective but slow, time-consuming and unhygienic. The increase in food demand has led to the invention of new technologies of grinding foods in lieu of the traditional methods. Such technologies include disc mills, which utilize attrition or shear forces for food grinding to achieve excellent ultrafine ground foodstuff (Bayram and Öner, 2007; Jung *et al*., 2018). Due to the high cost of imported grinding mills for food processing, locally fabricated mills, made of cast iron grinding discs, were developed (Yahaya *et al*., 2012). However, the tiny ridges, extending from edge to middle on their surface between the pair of the stationary and rotating disc mill, cause shear force during operation (Israila and Halima, 2016). A typical domestic grinding machine has two grinding discs. The constant friction causes the discs to wear out quickly (Kwofie and Chandler, 2007). The existing grinding discs have also poor wear resistance due to the materials used for their production; they have inadequate quality assurance to ascertain some of the critical engineering properties such as hardness and resistance to corrosion and wear.

The iron filings or metallic inclusion that contain heavy metals from the surface of the grinding discs contaminate the foods. The metallic contaminants go into and consequently harm the human body system. Iron filings, extracted from ground millet, are potential causes of hemochromatosis. Excess iron stored in human organs especially the liver, heart and pancreas can lead to life-threatening conditions such as liver disease, heart problems and diabetes (Shakiru and Babasola, 2014; Odusote *et al*., 2017). The growing health concern requires the improvement of the existing locally fabricated grinding discs to reduce the rate of iron filing contaminants. This will also improve the quality of ground food and reduce the frequency of regrooving or replacement of the grinding disc.

The alloying of the disc materials has been considered to increase their corrosion and wear resistance. Grey cast iron accounts for the most widely used material for local grinding disc due to its beneficial wear resistance under wet lubrication (Gupta *et al*., 2009; Atanda *et al*., 2010). Diesel engine block components are also sources of excellent thermal and vibration damping properties (Collini *et al*., 2008). Redesigning of existing grinding mills have been considered by using misalignment sensor and incorporation of permanent magnet and the utilization of steel as grinding media has been reported, which are expensive (Normanyo *et al*., 2009; Aldrich, 2013). Grey cast iron has carbon content varying between 2.5 and 4.0 wt.% and silicon content ranging between 1.0 and 3.0 wt.% with a slow cooling rate during

solidification. The composition of cast iron on the iron-carbon phase diagram reveals that it turns absolutely into liquid at a temperature between 1,150 and 1,300 °C. Therefore, it melts easily and is amenable to casting compared with steel (Callister, 2014).

Generally, wear resistance depends on matrix microstructure, carbide type characteristics (size, morphology, distribution and orientation), volume fraction, fracture toughness, hardness, loading conditions, features of tribological environments, relative movement of the contact surface, and type and size of the abrasive bodies (Agunsoye *et al*., 2014). Hardness, toughness and resistance to wear are crucial for the production of domestic grinding discs without compromising other properties. During solidification, high levels of chromium (Cr) lead to the formation of a high-volume fraction of eutectic carbides, which may or may not be associated with primary carbides in a heterogeneous austenitic/martensitic dendritic structure; however, the excellent abrasion resistance is mainly due to their presence (Scandian *et al*., 2009).

Agunsoye *et al*. (2013) characterized the abrasive wear properties of grey cast iron with silicon alloy where the wear performance was observed above 3.2% silicon addition. However, Cr ensures that austenite transforms to martensite at reduced temperatures (American Society for Metals International, 1996). To add Cr during casting, ferrochrome (FeCr) is usually used in practice but low silicon content is desired (Jalkanen and Gasik, 2013). Wear resistance has a clear linear correlation to increased hardness. Also, microstructure and chemical composition play a significant role in wear resistance.

Based on the reviewed literature, only a few investigations emphasized the improvement of the abrasive wear of the locally made grinding disc with gray cast iron utilizing FeCr and establishing its chemical constituent. This study considered the utilization of scrap engine block and recycled grinding disc as locally practiced with the addition of FeCr. The effect of FeCr addition on the wear properties of grey cast iron in the production of domestic grinding discs was investigated.

2. Methodology

2.1 Materials

The scraps were sourced from used local grinding discs and engine blocks. FeCr was obtained from Akure, Nigeria (Figure 1). Other materials were silica

sand (Shuaib-babata *et al*., 2017), clay binders, shovels, mold flasks, water, sieves, wire brushes, head pans and rammers. An infrared thermometer (BT-1500, BTMeter Instrument, China) was utilized for temperature measurement. A crucible furnace was used for this study.

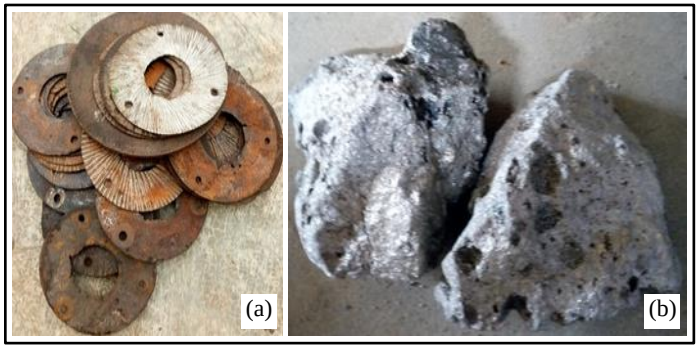

Figure 1. Scrap grinding disc (a) and FeCr used for casting of the specimens (b)

2.2 Mold Making

Green sand molding and casting operations were carried out at Hasbunallah Foundry, Ilorin, Kwara State, Nigeria. The molding consisted of four molding boxes and the patterns were arranged vertically inside. Foundry sand (mixture of clay, sieved sand and water) was first laid and rammed in the drag. The patterns were tapped in while subsequent molding boxes were filled and rammed appropriately until all the patterns were almost covered. The patterns were tapped and raised for easy removal. Pouring cups were shaped on each mold cavity as shown in Figure 2a.

2.3 Charging, Melting and Pouring

A pre-determined 40 kg of charge containing 60% engine block scraps and 40% grinding disc scraps were charged into the crucible furnace and heated to its pouring temperature (1,350 to 1,400 °C) with adequate fluidity check. An infrared thermometer was used to measure the tapping temperature. In Figure 2b, the molten metal in the crucible was poured into the mold without FeCr addition to produce the first batch: the control specimen was labeled with A.

Furthermore, a known charge weight of 1% of FeCr granules was added to the remaining molten melt in the crucible to increase the Cr content. This was thoroughly stirred to ensure homogenization, heated up to 1,370 °C and

poured into the next cavities labeled B for this specimen only. Subsequently, a known quantity of charge weight and 2, 3 and 4% of the charge weight of FeCr granule were melted to increase the Cr contents of the castings to produce specimens C, D and E, respectively.

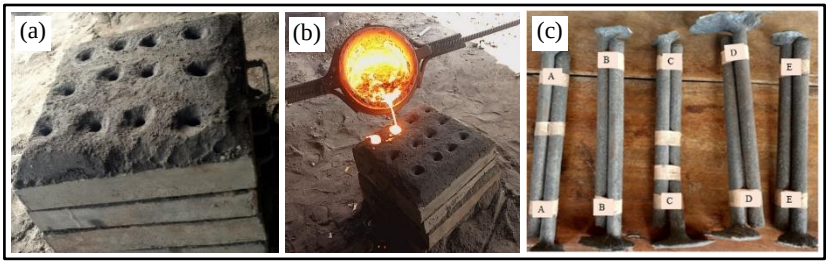

Figure 2. Green sand mold for cast iron specimen castings (a), pouring of molten metal into the mold (b) and cast rods for the mechanical test (c)

The Cr contents in the casts, thus, increased in succession. Adequate precautions to avoid defects in the castings were taken with a consistent pouring temperature of 1,370±30 °C, deslagging and returning the crucible into the furnace. The molds were left for the molten metal to solidify and cool at about 37 °C before the casting removal. The specimens were removed, sandblasted to eliminate sand grains and tagged appropriately for proper identification (Figure 2c).

2.4 Specimen Characterization

The specimens were sectioned and prepared (ground, polished and etched with 2% nital solution) for microstructural analysis using the American Society for Testing and Materials (ASTM) E3-11 (2011) standard procedure and adhering to graphite retention avoidance to obtain glassy surfaces (Radzikowska, 2005). The compositional analysis was carried out using optical emission spectroscopy (OES) (Spectromaxx LMF06, Agilent Scientific Instruments, United States) at Midwal Engineering Materials Testing Laboratory, Lagos, Nigeria. The ASTM A247-19 (2019) standard was followed for evaluation of microstructure at magnification bars of 20 µm with an optical microscope (BX60F-3, Olympus Optical Co., Japan) at the Universiti Teknologi Mara (UiTM) Material Science Laboratory, Malaysia. Scanning electron microscopy (SEM) (SU3500, Hi-Tech Instrument, Japan) equipped with an energy dispersive X-ray spectrometry (EDS) were carried out for the analytical identification of the element in the specimens. The phases present in the material were examined using an X-ray diffractometer (XRD) (Ultima IV, Rigaku, Japan) at UiTM, Malaysia. The hardness test was estimated based

on ASTM E10-15 (2015) using the Brinell hardness testing machine (Nexus 3200, Innovatest Europe BV., Netherlands). The pin on the disc wear machine was utilized to test the wear resistance specimens based on ASTM G99-05 (2010). The specimens with the dimension of 20-mm diameter and 40-mm height were pinned on the wear testing machine under the same load, speed and time. All specimens were weighed using a digital weighing balance (HX 302, Mettler Toledo, Switzerland) and were carefully cleaned with acetone before being re-weighed for net weight loss of each specimen. An average was computed from three tests conducted on each specimen. The abrading wheel was resurfaced after each specimen to avoid clogged surfaces and to reduce variation error. The wear index was calculated using Equation 1.

$$Wear\ index = \frac{Initial\ weight\ (W_1)\ - Final\ weight\ (W_2)}{RPM} \quad (1)$$

where *RPM* is equal to 100 rpm.

3. Results and Discussion

3.1 Specimen Composition

Cr was observed to increase with the addition of FeCr as shown in Table 1. Furthermore, the FeCr can be classified as high Cr and low carbon grade since the carbon wt.% was slightly maintained throughout the percentage addition in the specimens (Bergmann *et al*., 2016; Steenkamp, 2019). The percentage of Cr varied in each specimen based on the amount of charged alloying element. The unalloyed cast (specimen A) contained the least Cr. Concerning the wt.% of Cr content in the control specimen A, the relative change of Cr in specimen B showed a percentage difference of about 6.23% increment. Furthermore, increments of 220.47, 576.56 and 589.91% on specimens C, D, and E, respectively, were observed. A decrease in the proportion of Cr with respect to the amount of charged FeCr was identified after specimen C. This may be ascribed to the formation of complex carbides and chromite that may constitute a slag system, which exists when the Cr solubility limit in iron (Fe) is exceeded (Jacob *et al*., 2018). The EDS spectra for the specimens also confirmed the presence of identified elements as presented in Figure 3. The peaks of Cr were detected to increase from specimens A to D but decreased in specimen E.

Table 1. Composition of the cast specimens

Specimens	Elements (wt.%)										
	Fe	Cr	C	Si	Mn	P	S	Mo	Ni	Cu	Sn
			2.5-4.0 max	1.0-3.0 max	0.25-1.0 max	0.05-1.0 max	0.02- 0.25 max				
A	94.8	0.0674	2.920	1.440	0.424	0.0808	0.0669	0.0125	0.0208	0.0718	0.0114
B	95.0	0.0716	2.740	1.440	0.425	0.0773	0.0690	0.0107	0.0119	0.0734	0.0112
C	94.9	0.2160	2.760	1.450	0.410	0.0725	0.0459	0.0099	0.0197	0.0749	0.0109
D	94.1	0.4560	2.840	1.480	0.411	0.0779	0.0535	0.0105	0.0265	0.0765	0.0112
E	94.6	0.4650	2.710	1.460	0.415	0.0778	0.0545	0.0101	0.0222	0.0759	0.0108

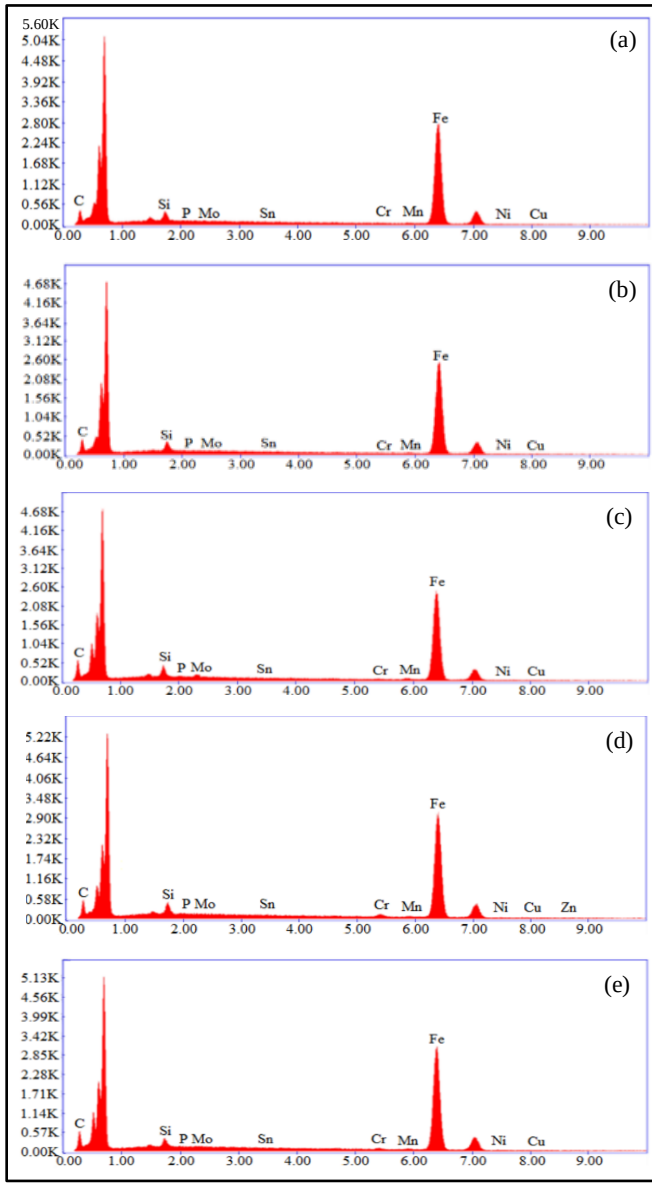

Figure 3. EDS spectra for specimen A unalloyed cast (a) and specimens B (b), C (c), D (d) and E (e) alloyed cast irons

3.2 X-ray Diffraction

The X-ray diffraction of the cast specimens is presented in Figure 4. The phases discovered vary relative to their composition. The Cr effect on the cast

iron was the focus of this present work. The peaks identification by miller indices for phases considered were FeC, Fe_5Si_3, FeCr and Fe_3C, which also corresponded to the peak list with reference codes 00-006-0686, 01-074-49750, 00-034-0396 and 03-065-0393, respectively. The presence of Fe predominated phase observed in specimen A was suppressed as the amount of Cr increased in specimens B through D (Huang *et al*., 2020).

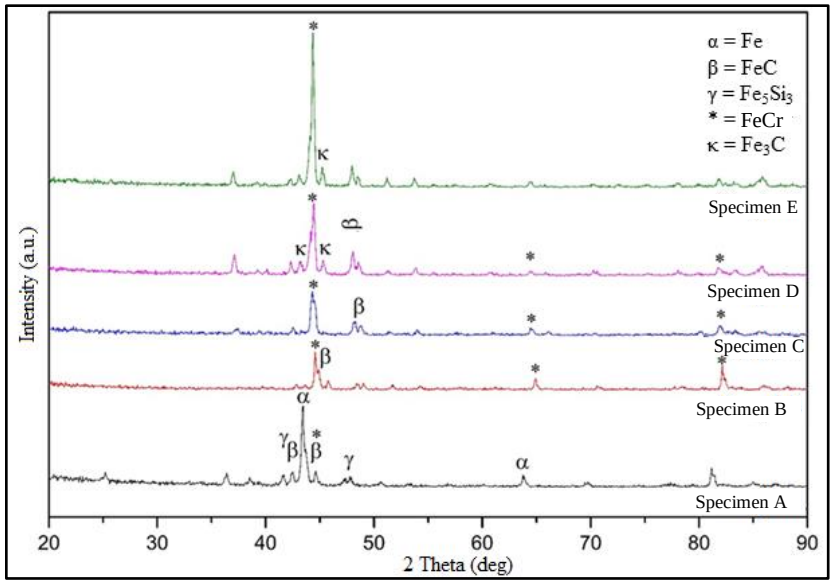

Figure 4. XRD patterns of unalloyed and FeCr-alloyed cast irons

The XRD spectra showed a slight increase in the overall intensity of the curve at low 2θ values, which indicated the presence of FeCr phases as prominent crystalline peaks, whose intensity increased along with the FeCr-added specimens. However, iron carbides were presented as either metastable FeC or stable cementite with an orthorhombic crystal structure. There was also a presence of iron silicide with hexagonal crystal structure in specimen A. This phase was replaced by more stable iron carbide phases due to the existence of carbide stabilizers. A comprehensive review has reported the various phases discovered in this study in the C-Cr-Fe system (Jacob *et al*., 2018). The low corresponding increment in Cr in specimen E might be a result of precipitation of chromium carbides, which reduced the amount of carbon. The excess Cr then formed chromium carbides that might lade the slag. Hence, a lower amount of Cr than expected from adding 366.35 g of FeCr.

3.3 Specimen Microstructure

The microstructures of the castings shown in Figure 5 represent the white cast iron (Abdel-Aziz *et al*., 2017; Wang and Yu, 2017; Kan *et al*., 2018; Li *et al*., 2018). Specimen A presented pearlite in a matrix of primary cementite but with spikes of primary FeCr. The addition of more Cr increased the amount of FeCr that was crystallized from pearlite and cementite. The formation of secondary FeCr commenced (Figure 5b). Figure 5c shows the precipitation of more primary iron chromite which, thereafter, increased with the addition of more Cr. The appearance of more dark phases and the disappearance of pearlite increased the network of cementite and FeCr, which was dispersed within the matrix of pearlite. The SEM images, presented in Figure 6, also revealed the same trend of carbide phases in the alloyed cast irons.

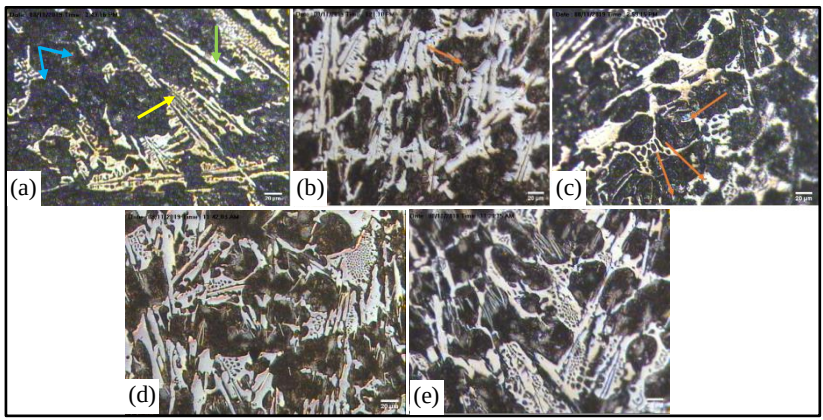

Figure 5. Optical microscopic examination of specimens A (a), B (b), C (c), D (d) and E (e) at magnification x20

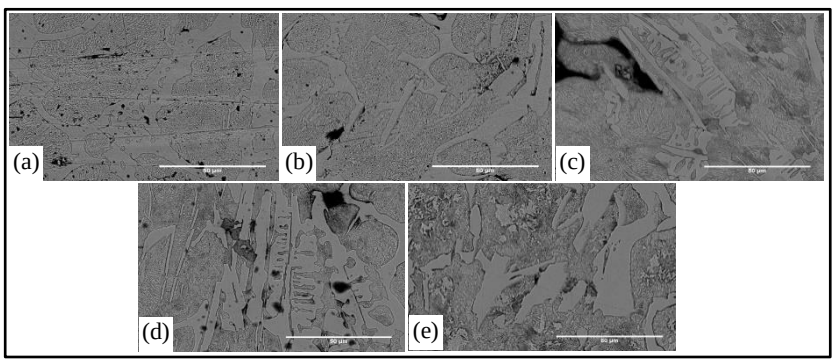

Figure 6. SEM images of specimens A (a), B (b), C (c), D (d) and E (e)

3.4 Specimen Wear Resistance

The average wear resistance testing conditions in this work were selected to represent the existing working conditions of grinding discs (Shakiru and Babasola, 2014). An increase in the silicon content in each of the specimen compositions reflected a decrease in wear index with the same test condition as illustrated in Figure 7. Specimen D showed the lowest wear index rate; a similar effect was reported in the literature (Agunsoye *et al*., 2013), wherein the effects of silicon additions improved the wear behavior of the grey cast iron. Furthermore, specimen D recorded the highest wt.% of silicon as presented in the elemental composition in Table 1.

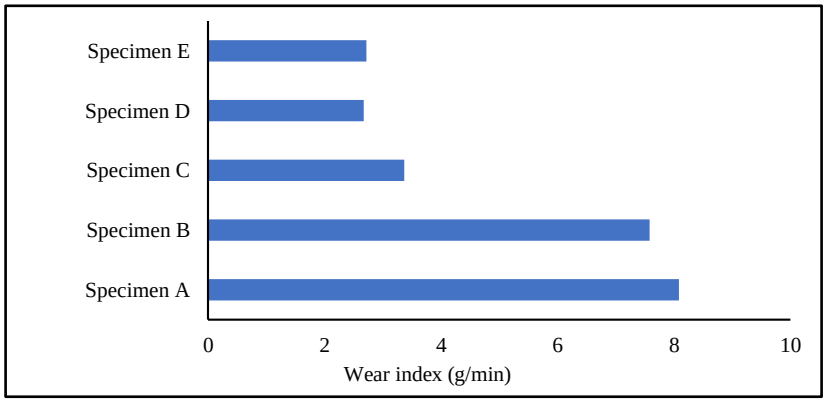

Figure 7. Variation in wear index of the specimens with varying percentage of FeCr

The wear index of the control specimen without FeCr (specimen A) was more than that of the other specimens with FeCr. The wear rate index (Figure 7) disclosed a progressive decrease towards higher Cr content specimens, which were much lower than that of the locally made control specimen A. However, specimen B with 0.0716 wt.% Cr had a 6% decrease in wear index compared with the control sample. Specimens C with 0.2160 wt.% Cr, D and E had 58, 67 and 66% decrease in wear index, respectively. The wear index of specimen D was less than that of specimen E, which may also be attributed to an increased stabilizing austenite element such as nickel and copper content present in specimen D than specimen E (Agunsoye *et al*., 2014; Medyński *et al*., 2019).

3.5 Specimen Hardness

The hardness values measured for all alloyed specimens showed higher Brinell hardness (BHN) than specimen A (Figure 8). The subsequent specimens showed a corresponding increment in hardness values with a proportion of Cr in the casts. The hardness values could be ascribed to the presence of FeCr carbides and precipitation of the secondary carbides with similar observation in Li *et al*. (2018). Concerning specimen A, the proportional increments observed in specimens B, C, D and E were 78.09, 91.49, 60.54 and 4.49%, respectively. This trend adequately showed that Cr increment increased the hardness value of the cast but with a limit of the maximum quantity – above which, the addition of Cr may show no corresponding effect. Hence, hardness increased relative to the FeCr addition and formation of the carbides.

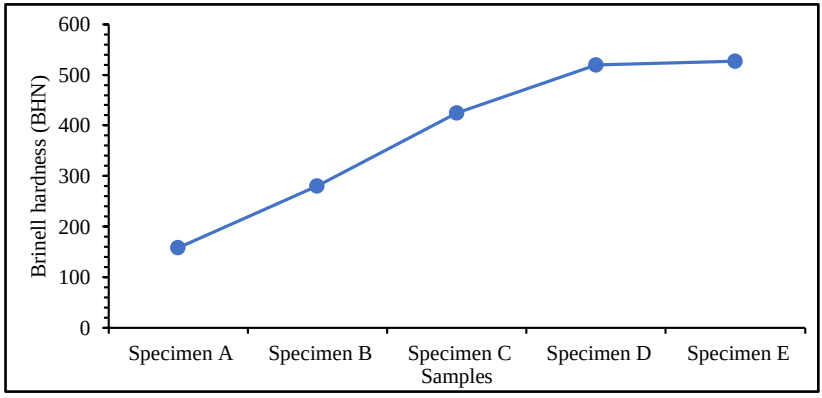

Figure 8. Brinell hardness of specimens A to E with varying percentage of FeCr addition

4. Conclusion and Recommendation

The wear resistance characteristics and hardness values of the produced alloyed specimens increased with the amount of FeCr in the grey cast iron. The presence of carbides was confirmed by the characterization techniques, thereby enhancing the hardness and wear resistance of the alloyed casts. Hence, the addition of FeCr to locally made grinding discs will reduce their wear rate and frequency of regrooving or replacement, and possibly decrease

the amount of metal wear during operation. In future work, the specimens can be adapted for impact load or other optimization techniques.

5. Acknowledgement

The authors wish to acknowledge the valuable contribution of Mr. Omotayo Sunday Awojobi of Materials and Metallurgical Engineering Department, University of Ilorin, Ilorin, Nigeria for his assistance in carrying out the foundry activities. No funding was received for this work.

6. References

Abdel-Aziz, K., El-Shennawy, M., & Omar, A.A. (2017). Microstructural characteristics and mechanical properties of heat treated high-Cr white cast iron alloys. International Journal of Applied Engineering Research, 12(14), 4675-4686.

Agunsoye, J.O., Bello, S.A., Hassan, S.B., Adeyemo, R.G., & Odii, J.M. (2014). The effect of copper addition on the mechanical and wear properties of grey cast iron. Journal of Minerals and Materials Characterization and Engineering, 02(05), 470-483. https://doi.org/10.4236/jmmce.2014.25048

Agunsoye, J.O., Isaac, T.S., Awe, O.I., & Onwuegbuzie, A.T. (2013). Effect of silicon additions on the wear properties of grey cast iron. Journal of Minerals and Materials Characterization and Engineering, 1(2), 61-67. https://doi.org/10.4236/jmmce.2013.12012

Aldrich, C. (2013). Consumption of steel grinding media in mills – A review. Minerals Engineering, 49, 77-91. https://doi.org/10.1016/j.mineng.2013.04.023

American Society for Metals International. (1996). ASM specialty handbook: Cast irons. Novelty, Ohio, United States: ASM International.

American Society for Testing and Materials (ASTM) A247-19. (2019). Standard test method for evaluating the microstructure of graphite in iron castings. West Conshohocken, PA: ASTM International.

American Society for Testing and Materials (ASTM) E10-15. (2015). Standard test method for Brinell hardness of metallic materials. West Conshohocken, PA: ASTM International.

American Society for Testing and Materials (ASTM) E3-11. (2011). Standard guide for preparation of metallographic specimens 1. West Conshohocken, PA: ASTM International.

American Society for Testing and Materials (ASTM) G99-05. (2010). Standard test method for wear testing with a pin-on-disk apparatus 1. West Conshohocken, PA: ASTM International.

Atanda, P., Okeowo, A., & Oluwole, O. (2010). Microstructural study of heat treated chromium alloyed grey cast iron. Journal of Minerals and Materials Characterization and Engineering, 09(03), 263-274. https://doi.org/10.4236/jmmce.2010.93021

Bayram, M., & Öner, M.D. (2007). Bulgur milling using roller, double disc and vertical disc mills. Journal of Food Engineering, 79(1), 181-187. https://doi.org/10.1016/j.jfoodeng.2006.01.042

Bergmann, C., Govender, V., & Corfield, A.A. (2016). Using mineralogical characterisation and process modelling to simulate the gravity recovery of ferrochrome fines. Minerals Engineering, 91, 2-15. https://doi.org/10.1016/j.mineng.2016.03.020

Callister, W.D. (2014). Materials science and engineering (9th ed.). New York: John Wiley & Sons.

Collini, L., Nicoletto, G., & Konečná, R. (2008). Microstructure and mechanical properties of pearlitic gray cast iron. Materials Science and Engineering A, 488(1-2), 529-539. https://doi.org/10.1016/j.msea.2007.11.070

Gupta, H.N., Gupta, R.C., & Arun, M. (2009). Manufacturing processes (2nd ed.). New Delhi, India: New Age International (P) Ltd., Publishers.

Huang, T.X., Li, Z., Huang, Y.Q., Li, Y., & Xiao, P. (2020). Microstructure and wear properties of SiC woodceramics reinforced high-chromium cast iron. Ceramics International, 46(3), 2592-2601. https://doi.org/10.1016/j.ceramint.2019.08.217

Israila, Y., & Halima, S. (2016). Effect of grinding plates (GUK, Parpela and Premier) on maize flour milled within Samaru, Nigeria. International Journal of Biochemistry Research & Review, 12(1), 1-7. https://doi.org/10.9734/ijbcrr/2016/2 1681

Jacob, A., Povoden-Karadeniz, E., & Kozeschnik, E. (2018). Revised thermodynamic description of the Fe-Cr system based on an improved sublattice model of the σ phase. Calphad: Computer Coupling of Phase Diagrams and Thermochemistry, 60, 16-28. https://doi.org/10.1016/j.calphad.2017.10.002

Jalkanen, H., & Gasik, M. (2013). Handbook of ferroalloys. In M. Gasik (Ed.), Theory of ferroalloys processing (pp. 29-82). Netherlands: Elsevier.

Jung, H., Lee, Y.J., & Yoon, W.B. (2018). Effect of moisture content on the grinding process and powder properties in food: A review. Processes, 6(6), 6-10. https://doi.org/10.3390/pr6060069

Kan, W.H., Albino, C., Dias-da-Costa, D., Dolman, K., Lucey, T., Tang, X., Chang, L., Proust, G., & Cairney, J. (2018). Microstructure characterisation and mechanical properties of a functionally-graded NbC/high chromium white cast iron composite. Materials Characterization, 136, 196-205. https://doi.org/10.1016/j.matchar.2017.12.020

Kwofie, S., & Chandler, H. (2007). Potential health effects of locally-manufactured corn-mill grinding plates. Journal of Science and Technology (Ghana), 26(2), 137-147. https://doi.org/10.4314/just.v26i2.32995

Li, Y., Li, P., Wang, K., Li, H., Gong, M., & Tong, W. (2018). Microstructure and mechanical properties of a Mo alloyed high chromium cast iron after different heat treatments. Vacuum, 156, 59-67. https://doi.org/10.1016/j.vacuum.2018.07.013

Medyński, D., Samociuk, B., Janus, A., & Checmanowski, J. (2019). Effect of Cr, Mo and Al on microstructure, abrasive wear and corrosion resistance of Ni-Mn-Cu cast Iron. Materials, 12(21), 3500. https://doi.org/10.3390/ma12213500

Normanyo, E., Asiam, E.K., Amankwa-Poku, K., & Adetunde, I.A. (2009). Redesign of a grinding mill for the minimisation of iron filings production. European Journal of Scientific Research, 36(3), 418-436.

Odusote, J.K., Soliu, G.A., Ahmed, I.I., Abdulkareem, S., & Akande, K.A. (2017). Assessment of metallic contaminants in grinded millet using domestic grinding machine. Nigerian Journal of Technological Development, 14(1), 13. https://doi.org /10.4314/njtd.v14i1.2

Radzikowska, J.M. (2005). Effect of specimen preparation on evaluation of cast iron microstructures. Materials Characterization, 54(4-5), 287-304. https://doi.org/10.1016 /j.matchar.2004.08.019

Scandian, C., Boher, C., de Mello, J.D.B., & Rézaï-Aria, F. (2009). Effect of molybdenum and chromium contents in sliding wear of high-chromium white cast iron: The relationship between microstructure and wear. Wear, 267(1-4), 401-408. https://doi.org/10.1016/j.wear.2008.12.095

Shakiru, O., & Babasola, D. (2014). Assessment of dry and wet milling using fabricated burr mill. Food Science and Quality Management, 31, 1-11.

Shuaib-babata, Y.L., Yaru, S. S., Abdulkareem, S., Ajayi, S., Busari, Y.O., Suleiman, A.K., Ibrahim, H.K., Ambali, I.O., & Mohammed, G.A. (2017). Suitability of some selected Ado-Ekiti (Nigeria) natural moulding sands' properties for sand casting. Covenant Journal of Engineering Technology, 1(2), 53-64.

Steenkamp, J.D. (2019). Wear analysis of tap-holes at two ferrochromium production furnaces. Journal of the Southern African Institute of Mining and Metallurgy, 119(6), 537-544. https://doi.org/10.17159/2411-9717/669/2019

Wang, H., & Yu, S. (2017). Influence of heat treatment on microstructure and sliding wear resistance of high chromium cast iron electroslag hardfacing layer. Surface and Coatings Technology, 319, 182-190. https://doi.org/10.1016/j.surfcoat.2017.04.013

Yahaya, D.B., Aremu, D.A., & Abdullahi, I. (2012). Investigation of metal contaminants in locally ground foods (beans and tomatoes). Journal of Emerging Trends in Engineering and Applied Sciences, 3, 339-343.